

Magnetic Behavior and Infrared Spectra of Jarosite, Basic Iron Sulfate, and Their Chromate Analogs

DANA A. POWERS*

*Division of Chemistry and Chemical Engineering, California Institute of Technology
Pasadena, California 91109*

GEORGE R. ROSSMAN

*Division of Geological and Planetary Sciences, California Institute of Technology,
Pasadena, California 91109*

HARVEY J. SCHUGAR

Department of Chemistry, Rutgers University, New Brunswick, New Jersey 08903

AND

HARRY B. GRAY*

*Division of Chemistry and Chemical Engineering, California Institute of Technology,
Pasadena, California 91109*

Received February 22, 1974

The magnetic behavior and infrared spectroscopic features of $\text{KFe}_3(\text{SO}_4)_2(\text{OH})_6$ (jarosite), $(\text{H}_3\text{O})\text{Fe}_3(\text{SO}_4)_2(\text{OH})_6$ (hydronium jarosite), $\text{KFe}_3(\text{CrO}_4)_2(\text{OH})_6$, $\text{Fe}(\text{OH})\text{SO}_4$ (basic iron sulfate) and $\text{Fe}(\text{OH})\text{CrO}_4$ (basic iron chromate) are reported. Spectroscopic data are in accord with X-ray data which show that $\text{KFe}_3(\text{SO}_4)_2(\text{OH})_6$, $(\text{H}_3\text{O})\text{Fe}_3(\text{SO}_4)_2(\text{OH})_6$, and $\text{KFe}_3(\text{CrO}_4)_2(\text{OH})_6$ are isostructural with $\text{KAl}_3(\text{SO}_4)_2(\text{OH})_6$ (akunite). All the species exhibit negative deviations from Curie-Weiss behavior over the temperature range 300–76°K. The compounds $\text{KFe}_3(\text{CrO}_4)_2(\text{OH})_6$ and $\text{Fe}(\text{OH})\text{CrO}_4$ undergo ferrimagnetic transitions at 73 and 71°K, respectively. Maxima occur in the susceptibilities of $\text{KFe}_3(\text{SO}_4)_2(\text{OH})_6$ and $(\text{H}_3\text{O})\text{Fe}_3(\text{SO}_4)_2(\text{OH})_6$ at 45 and 50°K.

Introduction

Magnetic studies of dimeric ferric complexes have shown that the extent of spin-interaction through a linear oxobridge is considerably greater than that through dihydroxy or dialkoxy bridges (1-3). These previous investigations have also identified infrared spectroscopic features which characterize the mode of bridging between ferric ions. We have extended these studies by examining polymeric,

extended-lattice, ferric compounds. Herein are reported the results for $\text{KFe}_3(\text{SO}_4)_2(\text{OH})_6$ (synthetic jarosite), $(\text{H}_3\text{O})\text{Fe}_3(\text{SO}_4)_2(\text{OH})_6$ (hydronium jarosite), $\text{KFe}_3(\text{CrO}_4)_2(\text{OH})_6$, $\text{Fe}(\text{OH})\text{SO}_4$ (basic iron sulfate) and $\text{Fe}(\text{OH})\text{CrO}_4$ (basic iron chromate).

Experimental

The following compounds were prepared by published procedures and characterized by

*Contribution No. 4839.

elemental analyses and X-ray powder diffraction patterns: $\text{Fe}(\text{OH})\text{SO}_4$, (4) calcd (%): Fe, 33.06; S, 56.87. Found: Fe, 32.85, 33.04; S, 57.03, 57.01. $\text{Fe}(\text{OH})\text{CrO}_4$ (5) calcd (%): Fe, 29.54; Cr, 27.54. Found: Fe, 29.15; Cr, 27.11. $\text{KFe}_3(\text{CrO}_4)_2(\text{OH})_6$ (5). Calcd (%): Fe, 30.99; Cr, 19.24; K, 7.23. Found: Fe, 30.77, 30.87; Cr, 18.95, 18.95; K, 6.99. $\text{KFe}_3(\text{SO}_4)_2(\text{OH})_6$ (6). Calcd (%): Fe, 33.45; S, 12.80, K, 7.81. Found: Fe, 33.41; S, 13.01, K, 7.68.

Two additional samples were used in this study: $(\text{H}_3\text{O})\text{Fe}_3(\text{SO}_4)_2(\text{OH})_6$, prepared by the method of Brauer (7). Calcd (%): Fe, 34.85; S, 13.40; K, 0.00. Found: Fe, 34.81; S, 13.55; K < 0.03; and a natural sample of $\text{KAl}_3(\text{SO}_4)_2(\text{OH})_6$ of Japanese origin, whose identity was confirmed by X-ray powder diffraction.

Partially deuterated analogs of the above species were obtained by using D_2O in place of H_2O as solvent in the preparative methods. Nearly completely deuterated samples of $\text{KFe}_3(\text{SO}_4)_2(\text{OH})_6$ and $\text{KFe}_3(\text{CrO}_4)_2(\text{OH})_6$ were prepared either from anhydrous reagents or from starting materials which had been recrystallized from D_2O . The deuterated species were characterized by X-ray powder diffraction, infrared spectroscopy, and optical microscopy.

Infrared spectra were taken on Perkin-Elmer Model 225 and Model 180 spectrophotometers using KBr and TlBr disks ($4000\text{--}200\text{ cm}^{-1}$) and paraffin wax films on polyethylene ($400\text{--}40\text{ cm}^{-1}$). Magnetic data were collected on a PAR Model FM-1 vibrating sample magnetometer calibrated with $\text{HgCo}(\text{SCN})_4$. Field strengths were measured with a Bell Model 600 A gaussmeter and Hall probe. Temperatures were measured with a Lakeshore Cryotronics GaAs diode or thermocouples calibrated against the diode. Magnetic and thermal data were collected with a maximum relative error of 1.0%. Diamagnetic corrections were taken from published data (8). X-ray powder diffraction patterns were obtained with a Debye-Scherrer Camera with film mounted in the Stramanis arrangement. Samples were mounted in 0.3 Glaskapillern tubes and subjected to rotation and recipro- cation during exposure to iron-filtered cobalt $\text{K}\alpha$ radiation.

Infrared Results and Absorption Band Assignments

The band positions in the infrared spectra of the compounds examined in this study are presented in Tables I and II. Spectra of $\text{KFe}_3(\text{SO}_4)_2(\text{OH})_6$, $\text{KFe}_3(\text{CrO}_4)_2(\text{OH})_6$, $\text{Fe}(\text{OH})\text{SO}_4$, and $\text{Fe}(\text{OH})\text{CrO}_4$ are shown in Fig. 1. Assignment of the bands in these spectra to specific structural motions is complicated by the extended-lattice nature of the species and the considerable overlapping of the absorptions, particularly for the sulfate-containing phases. It must be emphasized, therefore, that the following interpretation represents an attempt to pinpoint only the main vibrational features of the compounds under discussion.

The O-H stretch in $\text{KAl}_3(\text{SO}_4)_2(\text{OH})_6$ produces an intense absorption band at 3482 cm^{-1} and a weaker shoulder at 3502 cm^{-1} . The band due to $\nu(\text{OH})$ in the spectrum of $\text{KFe}_3(\text{SO}_4)_2(\text{OH})_6$ is a single intense peak at a somewhat lower energy (3385 cm^{-1}). Upon cooling to 93°K , doublet $\nu(\text{OH})$ structure is resolved, much like that observed in the spectrum of the aluminum phase. Deuteration shifts the main peak in the iron phase to 2510 cm^{-1} ($\nu_{\text{H}}/\nu_{\text{D}} = 1.35$).

The OH deformation in $\text{KFe}_3(\text{SO}_4)_2(\text{OH})_6$ is also at lower energy (1003 cm^{-1}) than its counterpart in the aluminum analog (1028 cm^{-1}). Deuteration shifts the absorption due to this deformation to 761 cm^{-1} ($\nu_{\text{H}}/\nu_{\text{D}} = 1.32$).

The infrared absorptions due to OH motions in the spectrum of $\text{KFe}_3(\text{CrO}_4)_2(\text{OH})_6$ are similar to those in the spectrum of the sulfate analog. The band attributable to OH stretching, which occurs at 3378 cm^{-1} , shifts to 2502 cm^{-1} ($\nu_{\text{H}}/\nu_{\text{D}} = 1.35$) with deuteration and resolves into a doublet when the sample is cooled to 93°K . The OH deformation gives rise to an absorption at 1002 cm^{-1} , which is shifted by deuteration to 742 cm^{-1} ($\nu_{\text{H}}/\nu_{\text{D}} = 1.35$).

The bands at 1181 and 1080 cm^{-1} in the spectrum of $\text{KFe}_3(\text{SO}_4)_2(\text{OH})_6$ are insensitive to deuteration and are assigned to components of the ν_3 mode of coordinated sulfate. The low site symmetry of SO_4^{2-} removes the degeneracy of the ν_3 mode and gives rise to the

TABLE I
INFRARED SPECTRA OF COMPOUNDS WITH ALUNITE STRUCTURE^a

$\text{KFe}_3(\text{CrO}_4)_2(\text{OH})_6$	$\text{KFe}_3(\text{CrO}_4)_2(\text{OD})_6$	$\nu_{\text{H}}/\nu_{\text{D}}$	$\text{KFe}_3(\text{SO}_4)_2(\text{OH})_6$	$\nu_{\text{H}}/\nu_{\text{D}}$	$\text{KFe}_3(\text{SO}_4)_2(\text{OD})_6$	$\nu_{\text{H}}/\nu_{\text{D}}$	$\text{Fe}_3(\text{SO}_4)_2(\text{OH})_6$ (H_3O^+)	$\text{KAl}_3(\text{SO}_4)_2(\text{OH})_6$	Assignment
3378 s	2502 s	1.35	3385 s	1.35	2510 s	1.35	3365 s	3502 shld } 3482 s }	O-H stretch HOH deformation ν_3 mode of SO_4^{2-}
1002 s	742 s	1.35	1635 ^c vw 1181 } 1080 }	1.35	1181 } 1080 } 1020 w 761 s	1.35	1632 s 1190 s 1085 s	1229 1090	ν_1 mode of SO_4 OH deformation
920 s } - } 850 s }	924 s } 890 ^b } 855 s }	0.99 0.99	1003 s	0.99		1.32	1002 s	1028 s	ν_3 mode of CrO_4^{2-}
568 w shld 495 s 437 s 412 shld 389 m } 348 m }	520 w 480 s 438 s 412 shld 390 m } 345 m }	1.09 1.03 1.00 1.00 1.00	650 shld } 626 s } 550 shld 505 s 469 s 441 vw	1.09 1.03 1.00 1.00	652 shld } 628 s }	0.98 1.00	650 shld } 616 s }	680 m } 627 s }	ν_4 mode of SO_4^{2-}
321 m 283 s 230 m 199 w 155 w	305 m 269 m 221 m	1.05 1.05 1.04	335 w 312 w 241 m 205 m 162 m 95 w	1.05 1.05 1.04	493 s 472 s 383 vw	1.02 0.99 1.15	505 s 465 s 440 shld	528 s 486 s 433 w	Vibrations of [FeO_6]oct ν_4 mode of CrO_4^{2-}
					335 w 309 w 245 m 205 m 162 m 95 m	1.00 1.01 0.98 1.00 1.00	341 m 306 w 250 w	360 m, sh 332 m 291 m 222 m 186 w 90 w	Vibrations of [FeO_6]oct and the remainder of the lattice

^a s = strong, m = medium, w = weak, vw = very weak, shld = shoulder, sh = sharp.

^b Impurity due to $\text{Fe}(\text{OH})\text{CrO}_4$.

^c Not present in all spectra but always weak when present.

TABLE II
INFRARED SPECTRA OF BASIC IRON SULFATE AND BASIC IRON CHROMATE^a

Fe(OH)(CrO ₄)	Fe(OD)CrO ₄	ν_{11}/ν_D	Fe(OH)SO ₄	Assignment
3418 s	2520	1.36	3458 s	OH stretch
			1172 s } 1138 s } 1112 s }	ν_3 motion of SO ₄ ²⁻
1027 s	745 s	1.38	1058 m	ν_1 motion of SO ₄ ²⁻
892 ss } 858 ss }	899 ss } 867 ss }	0.99	1020 s	OH deformation
				ν_3 motion of CrO ₄ ²⁻
			650 w } 638 s }	ν_4 motion of SO ₄ ²⁻
527 s	582 s	0.91	585 w } 538 s }	Vibrations of (FeO ₆) _{oct}
435 m	437 m	1.00	505 w } 468 m }	
			410 vw }	
395 w } 353 m }	400 w } 354 m }	0.99		ν_4 motion of CrO ₄ ²⁻
328 m	330 m	1.00		
296 s	301 s	0.98	331 s } 270 w }	Vibrations of (FeO ₆) _{oct}

^a s = strong, m = medium, w = weak, vw = very weak

two absorptions. Similar bands appear at 1229 and 1090 cm⁻¹ in the spectrum of KAl₃(SO₄)₂(OH)₆. The ν_3 mode of CrO₄²⁻ also produces two bands at 920 and 850 cm⁻¹ in the spectrum of KFe₃(CrO₄)₂(OH)₆. The ν_4 mode of sulfate is split by the low site symmetry to give a band at 626 cm⁻¹ and a shoulder at 650 cm⁻¹ in the spectrum of KFe₃(SO₄)₂(OH)₆. Similar bands appear at 626 and 680 cm⁻¹ in the spectrum of the aluminum analog. The bands at 389 and 348 cm⁻¹ in the spectrum of KFe₃(CrO₄)₂(OH)₆ are assigned to the ν_4 motion of CrO₄²⁻.

The low site symmetries of SO₄²⁻ and CrO₄²⁻ ought to make the ν_1 and ν_2 vibrational modes of these groups infrared active. In fully deuterated KFe₃(SO₄)₂(OH)₆ a sharp, but relatively weak, band at 1020 cm⁻¹ can be observed, and is assigned to the ν_1 motion. The assignment is based on the location of ν_1 vibrations of SO₄²⁻ in other compounds (9). The infrared spectrum of KFe₃(CrO₄)₂(OH)₆ does not exhibit any absorption attributable to ν_1 of CrO₄²⁻. The expected location of ν_1 of chromate, 830 cm⁻¹, may be obscured by absorption bands due to the ν_3 mode. No

bands in the spectra of any of the compounds could be assigned to the ν_2 mode of either SO₄²⁻ or CrO₄²⁻. In the case of CrO₄²⁻, absorption bands due to ν_2 would be obscured by absorptions attributable to the ν_4 mode. Coupling between the ν_2 mode of SO₄²⁻ and metal ion motion could shift a ν_2 absorption into a region of the spectrum where it could be obscured as well.

The remaining absorption bands are assigned to motions of the FeO₆ or AlO₆ coordination octahedron. Though considerable shifting of these absorptions occurs between iron and aluminum analogs, it was not possible to assign them more specifically.

The spectrum of (H₃O)Fe₃(SO₄)₂(OH)₆ is nearly identical to that of its potassium counterpart. Aside from an intensification of the ν (OH) band, the only new feature in the spectrum is the appearance of a moderately strong band at 1632 cm⁻¹. The spectra of all the other phases show at most only a very weak absorption in this region. All the weak absorptions are readily assignable to absorbed or entrained water. The band in the spectrum

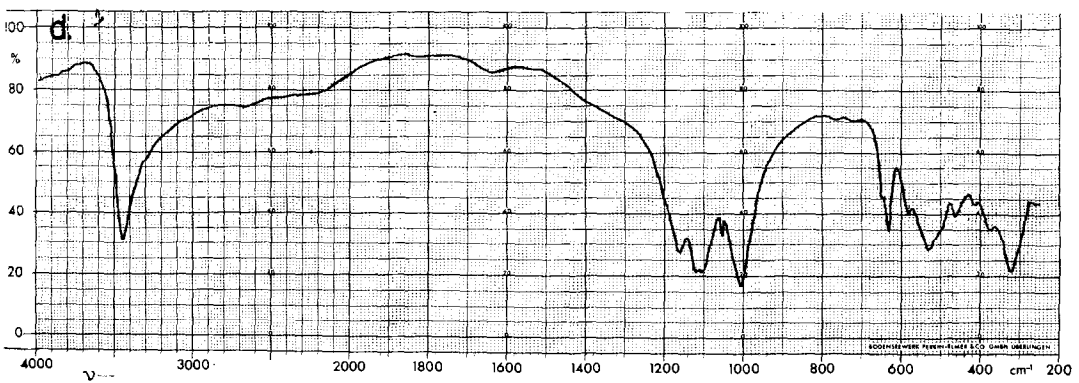
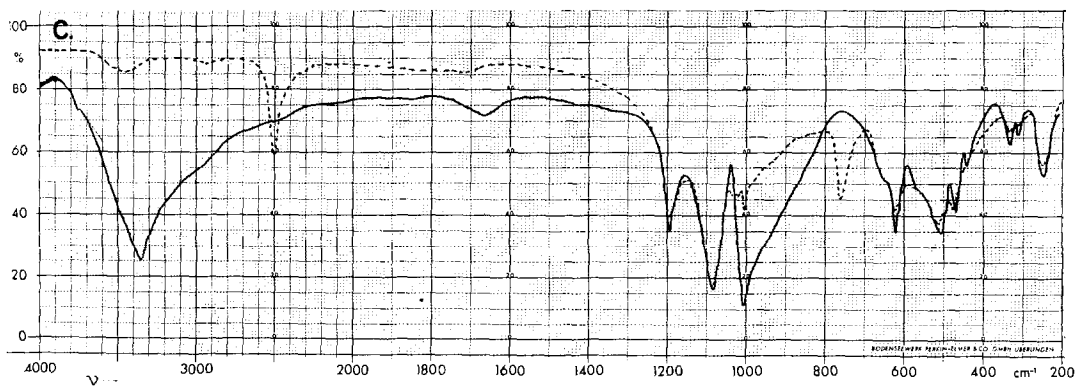
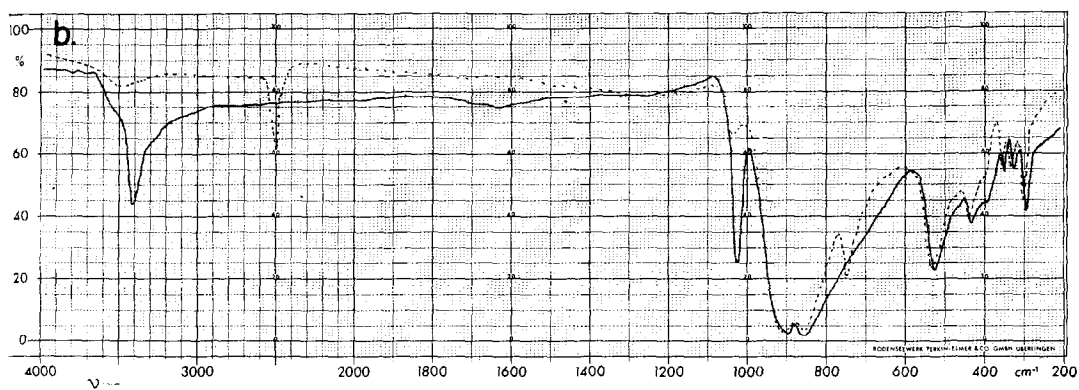
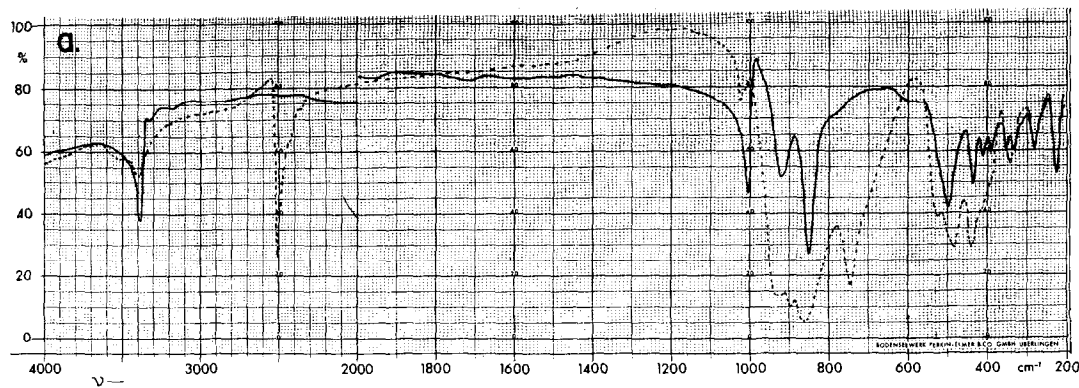


FIG. 1. Infrared spectra of (a) $\text{KFe}_3(\text{CrO}_4)_2(\text{OH})_6$, (b) $\text{Fe}(\text{OH})\text{CrO}_4$, (c) $\text{KFe}_3(\text{SO}_4)_2(\text{OH})_6$, and (d) $\text{Fe}(\text{OH})\text{SO}_4$. Dashed lines indicate spectra of deuterated species.

of $(\text{H}_3\text{O})\text{Fe}_3(\text{SO}_4)_2(\text{OH})_6$ cannot be so explained, and it could possibly be due to the HOH deformation of the hydronium cation.

The infrared spectra of $\text{Fe}(\text{OH})\text{CrO}_4$ and $\text{Fe}(\text{OH})\text{SO}_4$ are similar to those of $\text{KFe}_3(\text{CrO}_4)_2(\text{OH})_6$ and $\text{KFe}_3(\text{SO}_4)_2(\text{OH})_6$. However, the spectra do allow a clear differentiation among these phases. The absorptions owing to OH vibrational modes are consistently higher in energy in the former compounds. In $\text{Fe}(\text{OH})\text{SO}_4$, the band due to $\nu(\text{OH})$ occurs at 3458 cm^{-1} , and the $\delta(\text{OH})$ band is at 1020 cm^{-1} . In the spectrum of $\text{Fe}(\text{OH})\text{CrO}_4$, these bands are at 3418 and 1027 cm^{-1} , respectively.

The ν_3 mode of SO_4^{2-} in basic iron sulfate is split by the reduced site symmetry into bands at 1172 , 1138 , and 1112 cm^{-1} . Only two broad bands (892 and 858 cm^{-1}) could be resolved for the ν_3 mode of CrO_4^{2-} in the spectrum of basic iron chromate. The ν_4 mode of SO_4^{2-} produces absorption bands at 650 and 638 cm^{-1} , and analogous bands owing to chromate are at 395 and 353 cm^{-1} . The reduced site symmetry of SO_4^{2-} and CrO_4^{2-} would be expected to render the ν_1 and ν_2 modes infrared active, as well as removing the degeneracies of ν_3 and ν_4 . A weak band at 1058 cm^{-1} in the spectrum of $\text{Fe}(\text{OH})\text{SO}_4$ may be assigned to the ν_1 vibration. Because of the complex nature of the ir spectra, however, no other bands in the basic iron compounds could be assigned unambiguously to ν_1 or ν_2 . Other bands in the spectra are assigned to vibrations of the FeO_6 coordination octahedron.

The infrared spectra of samples cooled to 93°K display considerable intensification and resolution of the band attributable to $\nu(\text{OH})$. There is also some shifting of band positions to higher energies. Absorption bands owing to the deformation mode of bridging hydroxide are especially sensitive to temperature. Such acute sensitivity has previously been observed in hydroxy and alkoxy bridged dimers (1-3). The $\delta(\text{OH})$ bands resolve and shift 6 to 10 cm^{-1} higher in energy. Other absorption bands in the infrared spectra also show small shifts to higher energy when the samples are cooled.

The far-infrared spectra of $\text{KFe}_3(\text{CrO}_4)_2(\text{OH})_6$ and $\text{Fe}(\text{OH})\text{CrO}_4$ over the region 525 – 40 cm^{-1} were examined at several temperatures

below 72°K . This region was searched because it should be sensitive to structural perturbations which might be associated with the dramatic change in magnetic behavior of these species at low temperatures (*vide infra*). However, only a smooth continuation of the band shifts mentioned above was observed.

Magnetic Results

Representative magnetic data obtained in this study are presented in Table III. All of the samples have magnetic moments per iron of 3.4 to $3.8\ \mu_B$ at room temperature. These moments are considerably lower than the spin-only value of $5.92\ \mu_B$ for isolated ferric ion, and are indicative of extensive exchange interaction. All of the samples display a weakly temperature dependent magnetic susceptibility over the temperature range 300 – 76°K (Fig. 2). The effective magnetic moments drop substantially over this temperature range.

In the region 300 – 80°K basic iron sulfate and basic iron chromate exhibit negative deviations from Curie-Weiss behavior. Maxima in the susceptibilities of these compounds are difficult to determine precisely, because in each case the temperature range over which the magnetic transition occurs is very large. A maximum at 173°K was estimated for $\text{Fe}(\text{OH})\text{SO}_4$. That of $\text{Fe}(\text{OH})\text{CrO}_4$ is more difficult to determine, but appears to be considerably higher at 290°K . Neither compound obeys the Curie-Weiss law over any significant range of the temperatures examined.

The compounds $\text{KFe}_3(\text{CrO}_4)_2(\text{OH})_6$, $\text{KFe}_3(\text{SO}_4)_2(\text{OH})_6$, and $(\text{H}_3\text{O})\text{Fe}_3(\text{SO}_4)_2(\text{OH})_6$ obey the Curie-Weiss law ($\chi = C/(T - \theta_w)$) from 300 to 80°K with Weiss temperatures of about -800°K . The Weiss temperatures indicate extensive antiferromagnetic exchange interactions among the metal ions. Incorporation of these large, negative, Weiss temperatures in the computation of effective magnetic moments yields values of about $6.8\ \mu_B$. These large values suggest that the iron ions are in the $S = 5/2$ state, but that simple Weiss theory fails to compensate properly for the exchange interactions among the metal ions. The compounds behave magnetically over the temperature region 300 – 80°K as antiferromagnets above their Neél points. The magnetizations

TABLE III
 MAGNETIC DATA FOR HYDROXBRIDGED COMPOUNDS

Diamagnetic correction ^e	$\text{KFe}_3(\text{SO}_4)_2(\text{OH})_6$ $= -195 \times 10^{-6}$ cgs	$\text{KFe}_3(\text{CrO}_4)_2(\text{OH})_6$ $= -200 \times 10^{-6}$ cgs	$(\text{H}_3\text{O})\text{Fe}_3(\text{SO}_4)_2(\text{OH})_6$ $= -195 \times 10^{-6}$ cgs	$\text{Fe}(\text{OH})\text{SO}_4$ $= -62.0 \times 10^{-6}$ cgs	$\text{Fe}(\text{OH})\text{CrO}_4$ $= -64 \times 10^{-6}$ cgs
Temperature (°K)	$10^3 \chi'_M$	$10^3 \chi'_M$	$10^3 \chi'_M$	$10^3 \chi'_M$	$10^3 \chi'_M$
	$\mu_{\text{eff}}/\text{Fe}$	$\mu_{\text{eff}}/\text{Fe}$	$\mu_{\text{eff}}/\text{Fe}$	$\mu_{\text{eff}}/\text{Fe}$	$\mu_{\text{eff}}/\text{Fe}$
298	15.8	13.7	15.1	6.11	5.06
250	16.1	14.2	15.7	6.26	5.04
200	16.8	14.7	16.3	6.34	4.97
150	17.7	15.3	16.9	6.32	4.85
100	18.6	16.0	17.8	6.14	4.66
50	19.8	75.4 ^b	19.7	5.89	13.06 ^b
15	18.1	81.8	18.0	6.00	15.56 ^b
θ_{Weiss}	$-770 \pm 100^\circ\text{K}$	$-770 \pm 100^\circ\text{K}$	$-840 \pm 100^\circ\text{K}$	^a	^a
θ_{Neel}	$45 \pm 10^\circ\text{K}$	^b	$50 \pm 10^\circ\text{K}$	$173 \pm 10^\circ\text{K}$	$290 \pm 40^\circ\text{K}$
$\mu^{298}\text{K}^c$	6.69	6.80	6.78	^a	^a

^a Does not obey Curie-Weiss Law.

^b Not a simple antiferromagnet—See text.

^c From $\mu_{\text{eff}}^0 = 2.828 [\chi'_M (T - \theta_m)]^{1/2}$.

^d From $\mu_{\text{eff}} = 2.828 [\chi'_M T]^{1/2}$.

^e From Ref. (8).

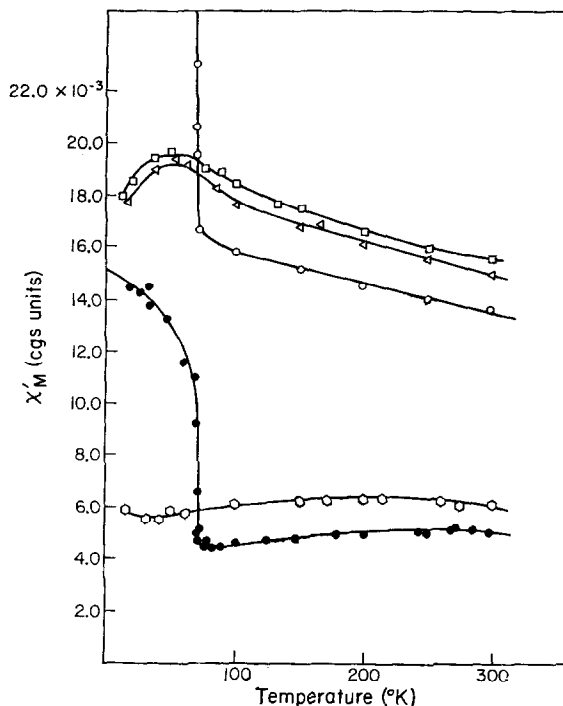


Fig. 2. Molar susceptibility vs temperature for \circ $\text{KFe}_3(\text{CrO}_4)_2(\text{OH})_6$, \triangle $(\text{H}_3\text{O}^+)\text{Fe}_3(\text{SO}_4)_2(\text{OH})_6$, \square $\text{KFe}_3(\text{SO}_4)_2(\text{OH})_6$, \diamond $\text{Fe}(\text{OH})\text{SO}_4$, and \bullet $\text{Fe}(\text{OH})\text{CrO}_4$.

vary linearly with applied field up to 11,000 Oe, and pass through zero at zero applied field.

The compounds $\text{KFe}_3(\text{SO}_4)_2(\text{OH})_6$ and $(\text{H}_3\text{O})\text{Fe}_3(\text{SO}_4)_2(\text{OH})_6$ have sharp maxima in their susceptibilities at 45 and 50°K, respectively. Small increases in the magnetic susceptibilities of these species at the lowest temperature are probably due to paramagnetic impurities. On the other hand, the chromate phases undergo abrupt changes in magnetic behavior in the lower temperature region. At 71 and 73°K, respectively, the magnetic susceptibilities of $\text{Fe}(\text{OH})\text{CrO}_4$ and $\text{KFe}_3(\text{CrO}_4)_2(\text{OH})_6$ rise sharply (Fig. 3). These transitions occur over a temperature range of less than 2°K. Once the transition occurs, the magnetization of each of these species displays saturation effects: $\text{KFe}_3(\text{CrO}_4)_2(\text{OH})_6$ is magnetically soft and its magnetization loop has no hysteresis losses ($H_c < 10$ Oe) (Fig. 4). Reversal of the magnetization once the applied field is reversed, however, is quite slow, requiring 3 hr to accomplish, at -80 Oe and

63°K. On a shorter time scale, hysteresis losses appear and the magnetization loop is considerably distorted from the centrosymmetric form. $\text{Fe}(\text{OH})\text{CrO}_4$ is extremely hard magnetically. Its magnetization loop shows huge hysteresis losses (Fig. 5). The coercive field is 7000 Oe at 55°K and greater than 11,000 Oe at 29°K. The magnetization loop of $\text{Fe}(\text{OH})\text{CrO}_4$ is severely distorted along the magnetization (M) axis as well as along the applied field (H) axis. Even at the highest field used in this study (11,000 Oe), $\text{Fe}(\text{OH})\text{CrO}_4$ did not saturate. It is possible that the hysteresis loop of basic iron chromate is a minor loop, which would account for its distorted, wasp-waisted form (10).

When samples of $\text{KFe}_3(\text{CrO}_4)_2(\text{OH})_6$ are contaminated with small amounts of $\text{Fe}(\text{OH})\text{CrO}_4$, they also have magnetization loops distorted along the M and H axes. It may be noted that Watanabe (11) observed similar behavior in LaFeO_3 contaminated with a magnetically hard impurity.

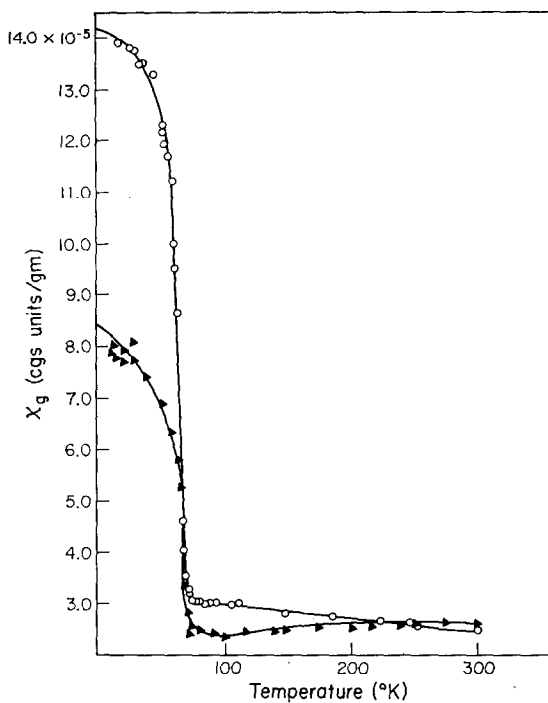


FIG. 3. Gram susceptibility vs temperature for ○ $\text{KFe}_3(\text{CrO}_4)_2(\text{OH})_6$, ▲ $\text{Fe}(\text{OH})\text{CrO}_4$.

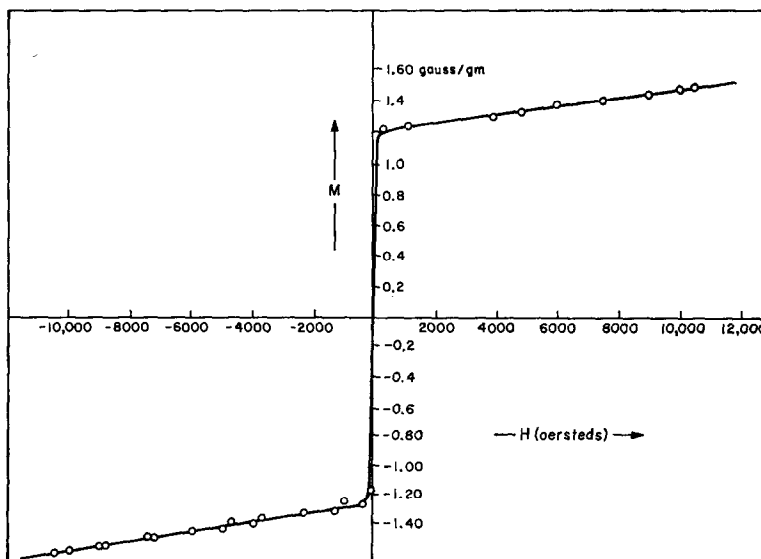


FIG. 4. Gram magnetization vs applied field (H) for $\text{KFe}_3(\text{CrO}_4)_2(\text{OH})_6$ at 28 $^{\circ}$ K.

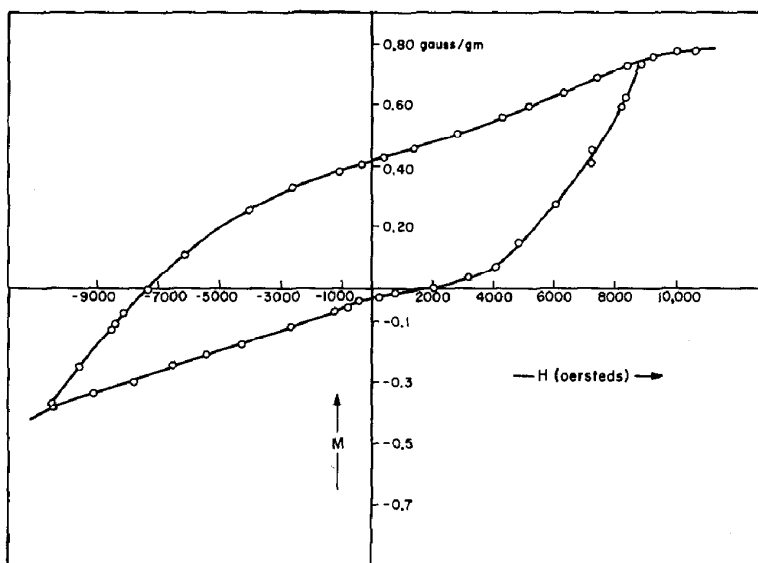


FIG. 5. Gram magnetization vs applied field (H) at 33°K for Fe(OH)CrO_4 .

Saturation magnetizations for both chromate phases indicate a magnetic moment ($n = \sigma_{0,\infty} MW / \beta N_A$) of only $0.05 \mu_B$, which is some 1000 times smaller than the nominally expected value for ferromagnetic ferric ($S = 5/2$) ions.

Discussion

The infrared spectra are in accord with the X-ray powder diffraction data, which show that $\text{KFe}_3(\text{CrO}_4)_2(\text{OH})_6$, $(\text{H}_3\text{O})\text{Fe}_3(\text{SO}_4)_2$ -

$(\text{OH})_6$, $\text{KFe}_3(\text{CrO}_4)_2(\text{OH})_6$, and $\text{KAl}_3(\text{SO}_4)_2(\text{OH})_6$ are isostructural. This structure (Fig. 6) consists of metal ions located in slightly distorted octahedral coordination polyhedra; each polyhedron has four-bridging hydroxides in a plane and sulfate or chromate oxygens at the apices (12). Three of the sulfate or chromate oxygens are coordinated to metal ions and the symmetry of the SO_4^{2-} or CrO_4^{2-} groups is reduced to C_s . The metal ions are joined together by the sulfate or chromate groups and the network of dihydroxy bridges

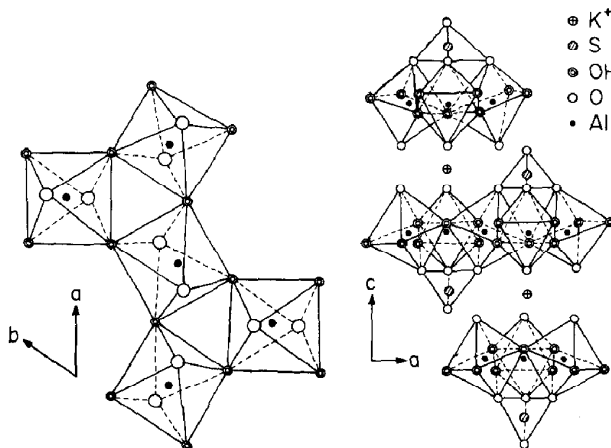


FIG. 6. Structure of $\text{KAl}_3(\text{SO}_4)_2(\text{OH})_6$ viewed along the a axis and viewed along the c axis (Wang (12)).

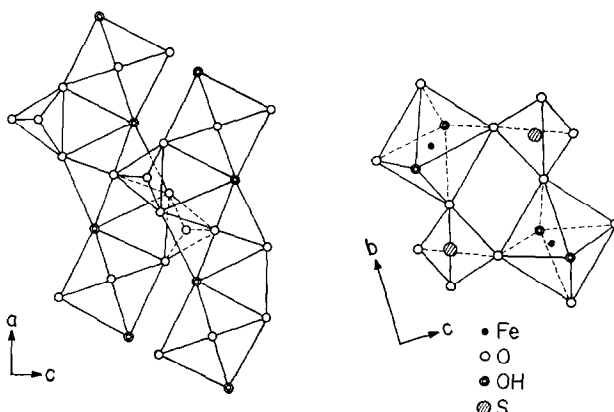


FIG. 7. Structure of Fe(OH)SO_4 viewed along the a axis and viewed along the b axis (Johansson (4)).

to form sheets separated by the uncoordinated sulfate or chromate oxygens and the cations, K^+ or H_3O^+ .

The infrared spectra also are consistent with the X-ray powder diffraction results of Bounin and Lecerf (5), which show that Fe(OH)CrO_4 has a structure very similar to that of basic iron sulfate. In this structure (Fig. 7) ferric ions in distorted octahedral coordination polyhedra form polymeric chains. The metal ions are linked by two, *trans* hydroxy bridges and coordinated sulfate or chromate oxygens. All sulfate and chromate oxygens are coordinated and the symmetries of the SO_4^{2-} and CrO_4^{2-} groups are reduced to C_s . The chains are linked together by coordinated sulfate or chromate groups (4).

The reduction in symmetry of the ideally tetrahedral chromate and sulfate is reflected in the infrared spectra. Vibrations due to the ν_3 and ν_4 modes, which are infrared active in T_d symmetry, are no longer degenerate and produce several absorption bands in the infrared spectra of all of the phases. In the spectra of the sulfate-containing phases, an absorption band may be assigned to $\nu_1(\text{SO}_4)^{2-}$, which is inactive in T_d symmetry.

The band assigned to HOH deformation in the infrared spectrum of $(\text{H}_3\text{O})\text{Fe}_3(\text{SO}_4)_2(\text{OH})_6$ provides some evidence for (H_3O^+) as a valid structural entity in this compound. However, the differences in the spectral results obtained for this species and those expected for coordinated or lattice water are not great

enough to allow a firm conclusion on this question.

The infrared spectra allow some improvement in the structural characterization of OH in these phases. The infrared band position of the O-H stretch is sensitive to hydrogen bonding interaction and may be used as a spectral ruler for hydrogen bond lengths (13). All hydrogen bonds were assumed to be linear, in keeping with the known structures of Fe(OH)SO_4 and $\text{KAl}_3(\text{SO}_4)_2(\text{OH})_6$. The hydrogen bond length calculated for $\text{KAl}_3(\text{SO}_4)_2(\text{OH})_6$ is $3.00 \pm 0.03 \text{ \AA}$, which is in excellent agreement with the value of 2.96 \AA found in a structural determination by Wang et al. (12). Our calculation leads us to prefer this structural determination over an older one (14), which found a hydrogen bond length of only 2.50 \AA . The hydrogen bond lengths calculated for $\text{KFe}_3(\text{SO}_4)_2(\text{OH})_6$ and $\text{KFe}_3(\text{CrO}_4)_2(\text{OH})_6$ are both $2.90 \pm 0.02 \text{ \AA}$. The only available structural information concerning basic iron sulfate reports that there is no hydrogen bonding (4). However, we calculate that the hydrogen bond lengths for basic iron sulfate and basic iron chromate are 2.87 and 2.84 \AA , respectively.

The spin structure of $\text{KFe}_3(\text{SO}_4)_2(\text{OH})_6$ has been treated theoretically as consisting of magnetically isolated sheets with ferric ions in a kagome array (15, 16). The basic iron sulfate structure has been treated as a collection of magnetically isolated infinite chains (17). Since the chromate and sulfate phases are

isostructural, and above their respective transition temperatures the magnetic behavior is quite similar, $\text{Fe}(\text{OH})\text{CrO}_4$ and $\text{KFe}_3(\text{CrO}_4)_2(\text{OH})_6$ can be treated in ways analogous to those used for their sulfate counterparts. These theoretical results require that magnetic exchange occur only between nearest-neighbor metal ions within the chain or sheet. The reduction in the effective magnetic moment from the value expected for isolated ferric ($S = 5/2$) ion is then a good indication of the strength of the antiferromagnetic coupling between the metal ions.

An interesting comparison between the temperature behavior of the effective magnetic moments of these polymeric species and that of moments for octahedrally coordinated ferric ions in various states of aggregation is shown in Fig. 8. Magnetically isolated ferric ions have temperature independent magnetic moments of $6.0 \mu_B$. Ferric dimers which are antiferromagnetically coupled through dihydroxy bridges have "reduced" 300°K moments of $5.1 \mu_B$ per iron. This moment drops to $1.0 \mu_B$ at 17°K. Oxobridged iron(III) dimers at 300°K have even lower moments of about $2.0 \mu_B$, indicative of the stronger antiferromagnetic coupling between the two metal ions. The effective moments for these oxobridged species drop to near zero at 30°K. The moments for

the polymeric species in this study lie between those for the hydroxy bridged dimers and the oxobridged ones. The availability of interaction with more than one nearest neighbor metal ion makes exchange through the hydroxy bridges of the polymeric species more extensive than in the simple dimeric compounds, but not so effective as exchange through a linear oxobridge. Closer examination of the data shows that the moment for $\text{Fe}(\text{OH})\text{SO}_4$ is somewhat higher than the moment for $\text{KFe}_3(\text{SO}_4)_2(\text{OH})_6$. Similarly, $\text{Fe}(\text{OH})\text{CrO}_4$ has a higher moment than $\text{KFe}_3(\text{CrO}_4)_2(\text{OH})_6$. In the basic iron sulfate structure each metal ion can interact magnetically with only two nearest neighbor metal ions, whereas in the alunite structure a metal ion can interact with either three or four nearest neighbors. Consequently, exchange is less effective in the basic iron sulfate structure and the magnetic moment should be, as is observed, higher than for compounds with the alunite structure. Chromate-containing species also have enhanced exchange interactions in the 300–80°K temperature range relative to species containing sulfate. Chromate ion possibly introduces small changes in the bond lengths and angles in the coordination polyhedra surrounding the metal ions. The differences between chromate and sulfate

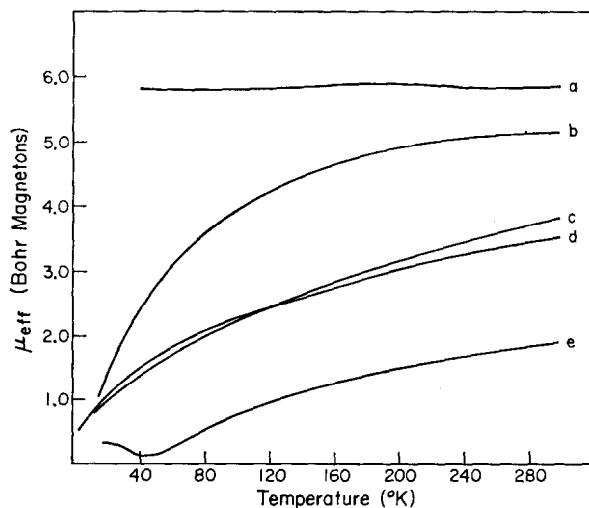


FIG. 8. μ_{eff} vs temperature for (a) $\text{Fe}(\text{picolinate})_2(\text{H}_2\text{O})\text{Cl}$, (b) $[\text{Fe}(\text{picolinate})_2(\text{OH})_2]_2$, (c) $\text{Fe}(\text{OH})\text{SO}_4$, (d) $\text{KFe}_3(\text{SO}_4)_2(\text{OH})_6$, (e) $\text{enH}_2[(\text{FeHEDTA})_2\text{O}] \cdot 6\text{H}_2\text{O}$.

manifest themselves most clearly in the magnetic behavior below 76°K, where the chromate-containing species exhibit ferrimagnetic behavior, whereas those with sulfate remain antiferromagnetic. The magnetic transition made by $\text{Fe}(\text{OH})\text{CrO}_4$ and $\text{KFe}_3(\text{CrO}_4)_2(\text{OH})_6$ does not mark a first-order phase change. The infrared spectra of these compounds are virtually identical at temperatures above and below their transition points. The transition points are correctly the Curie points of these phases.

The saturation magnetizations of $\text{Fe}(\text{OH})\text{CrO}_4$ and $\text{KFe}_3(\text{CrO}_4)_2(\text{OH})_6$ are quite low, reminiscent of so-called weak ferromagnetism. Weak ferromagnetism is a poorly understood phenomenon which has been reviewed by Moriya (18). Compounds that are weakly ferromagnetic typically have very sharp transition points, and above the transition point follow Curie-Weiss behavior with large, negative Weiss temperatures. A variety of mechanisms, such as defects in stoichiometry (19), antiferromagnetic domains with magnetized walls, grain boundary interactions (20), or the intrinsic nature of the material (18, 21, 22) have been invoked to explain the occurrence of weak ferromagnetism. It is difficult to choose among these possible mechanisms. Rationalizing the onset of weak ferromagnetism based on spin configurations is attractive, as both the chromate phases develop well-formed, though small, crystals and their magnetic properties vary little from sample to sample. It is well known that a linear chain of spins cannot develop stable ferromagnetism (23). The approximation that treats basic iron chromate as linear, independent, chains of ferric ions must fail below 73°K. Takano et al. (15) proposed that metal ions in a kagome array, such as in $\text{KFe}_3(\text{SO}_4)_2(\text{OH})_6$ and $\text{KFe}_3(\text{CrO}_4)_2(\text{OH})_6$, could adopt a stable antiferromagnetic structure only with a triangular spin arrangement. In a colinear spin arrangement, the metal ions in a kagome array could develop stable ferromagnetism. Thus, a possible interpretation of our results is that the onset of weak ferromagnetism in $\text{KFe}_3(\text{CrO}_4)_2(\text{OH})_6$ marks the change from a triangular to a colinear spin arrangement.

The sharp onset of ferromagnetism and the

differences in the magnetic behavior of basic iron chromate and $\text{KFe}_3(\text{CrO}_4)_2(\text{OH})_6$, are subjects of intensive investigation in these laboratories.

Acknowledgments

Dana A. Powers would like to thank the Fannie and John Hertz Foundation for the award of a fellowship. This research was supported by the National Science Foundation.

References

1. H. J. SCHUGAR, G. R. ROSSMAN, AND H. B. GRAY, *J. Amer. Chem. Soc.* **91**, 4564-66 (1969).
2. H. J. SCHUGAR, G. R. ROSSMAN, C. G. BARRACLOUGH, AND H. B. GRAY, *J. Amer. Chem. Soc.* **94**, 2683-90 (1972).
3. C. -H. S. WU, G. R. ROSSMAN, H. B. GRAY, G. S. HAMMOND, AND H. J. SCHUGAR, *Inorg. Chem.* **11**, 990-994 (1972).
4. G. JOHANSSON, *Acta Chem. Scand.* **16**, 1234 (1962).
5. A. BOUNIN AND A. LERCERF, *Comp. Rend. Ser. C.* **262**, 1782 (1966).
6. J. G. FAIRCHILD, *Amer. Mineral.* **18**, 543 (1933).
7. G. BRAUER (Ed.), "Handbook of Preparative Inorganic Chemistry," 2nd ed., p. 1507, 1965.
8. P. W. SELWOOD, "Magnetochemistry," 2nd ed., Interscience New York, 1956.
9. K. NAKAMOTO, "Infrared Spectra of Inorganic and Coordination Compounds," 2nd ed., Wiley Interscience, New York, 1970.
10. I. S. JACOBS AND C. P. BEAN, In "Magnetism," (G. T. Rado and Harry Suhl, Eds.) Vol. III, Chap. 6, Academic Press, New York, 1963.
11. H. WATANABE, *J. Phys. Soc. Japan* **14**, 511 (1959).
12. R. WANG, W. F. BRADLEY, AND H. STEINFINK, *Acta Cryst.* **18**, 249 (1965).
13. K. NAKAMOTO, M. MARGOSHES, AND R. E. RUNDLE, *J. Amer. Chem. Soc.* **77**, 6480 (1959).
14. S. B. HENDRICKS, *Amer. Mineral.* **22**, 773 (1937).
15. M. TAKANO, T. SHINJO, AND T. TAKADA, *J. Phys. Soc. Japan* **30**, 1049-53 (1971).
16. I. SOYOZI, *Prog. Theor. Phys.* **6**, 306 (1951).
17. R. W. CATTRALL, K. S. MURRAY, AND K. I. PEVERILL, *Inorg. Chem.* **10**, 1301 (1971).
18. T. MORIYA, In "Magnetism" (G. T. Rado and H. Suhl, Eds.), Vol. I, Chapt. 3. Academic Press, New York, 1963.
19. L. NEÉL, *Ann. Phys. Ser. 4*, 249 (1949).
20. Y. Y. LI, *Phys. Rev.* **101**, 1450 (1956).
21. I. DZYALOSHINSKY, *J. Phys. Chem. Solids* **4**, 241 (1958).
22. I. S. JACOBS AND C. P. BEAN, *J. Applied Phys.* **29**, 537 (1958).
23. J. H. VAN VLECK, *Rev. Mod. Phys.* **17**, 34 (1945).